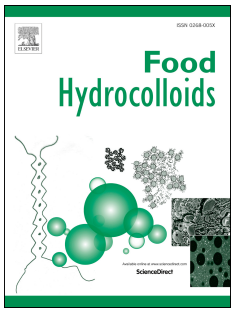

Preparation of cinnamon essential oil emulsion by bacterial cellulose nanocrystals and fish gelatin

Mahsa Sadat Razavi, Abdollah Golmohammadi, Ali Nematollahzadeh, Filippo Fiori, Cesare Rovera, Stefano Farris

PII: S0268-005X(20)30207-1

DOI: https://doi.org/10.1016/j.foodhyd.2020.106111

Reference: FOOHYD 106111

To appear in: *Food Hydrocolloids*

Received Date: 26 January 2020

Revised Date: 1 June 2020

Accepted Date: 15 June 2020

Please cite this article as: Razavi, M.S., Golmohammadi, A., Nematollahzadeh, A., Fiori, F., Rovera, C., Farris, S., Preparation of cinnamon essential oil emulsion by bacterial cellulose nanocrystals and fish gelatin, *Food Hydrocolloids* (2020), doi: https://doi.org/10.1016/j.foodhyd.2020.106111.

Graphical abstract

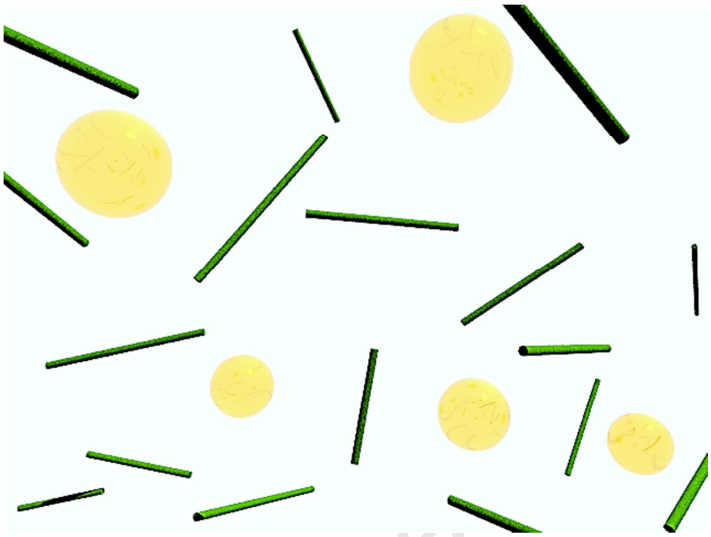

Preparation of cinnamon essential oil emulsion by bacterial cellulose nanocrystals and fish gelatin

Mahsa Sadat Razavi[1], Abdollah Golmohammadi[1], Ali Nematollahzadeh[2], Filippo Fiori[3], Cesare Rovera[3], Stefano Farris[3*]

[1] *Department of Biosystems Engineering, University of Mohaghegh Ardabili, P.O. Box 179, Ardabil, Iran*

[2] *Department of Chemical Engineering, University of Mohaghegh Ardabili, P.O. Box 179, Ardabil, Iran*

[3] *DeFENS, Department of Food, Environmental and Nutritional Sciences, Food Packaging Lab, University of Milan, via Celoria 2 – I-20133 Milan, Italy*

***Corresponding author**

Tel.: +39 0250316805; Fax: +39 0250316672

Email address: stefano.farris@unimi.it (S. Farris)

Abstract

This study was aimed at preparing nanoemulsions with bacterial cellulose nanocrystals (BCNCs) and cinnamon essential oil (CEO) with and without fish gelatin. The effect of CEO concentration (0.2, 0.4, 0.8, 1.57, 2.34 and 3.1% v/w) and pH (3.5 and 5) on the droplet size, ζ-potential, morphology, and encapsulation efficiency (EE) of CEO/BCNC emulsions was investigated. It was observed that ζ-potential was approximately -25 mV for the BCNC emulsions, whereas it changed to positive values (from approximately 4 mV to 12 mV) in the systems containing gelatin (3% w/w). In addition, in the presence of gelatin, emulsions exhibited larger droplets (450-1000 nm) than did the CEO/BCNC emulsions (350-550 nm), as demonstrated by transmission electron microscopy. TEM analysis also revealed the surfactant activity of gelatin, which displaced between the hydrophobic CEO nanodroplets and the more polar BCNCs. The effect of pH on EE was significant for the emulsions in the presence of gelatin in that EE was higher at pH 5 than at pH 3.5 up to a CEO concentration of 0.24% w/v. Finally, a direct relationship was established between CEO concentration and EE for emulsions with and without gelatin.

Keywords: bacterial cellulose nanocrystals; essential oil; fish gelatin; stabilization.

Introduction

Essential oils (EOs) extracted from plants (e.g., cinnamon, thyme, oregano, and clove) have inherent antimicrobial properties, including inhibiting the growth of bacteria, yeasts, and fungi. For this reason, their potential use to prolong the shelf life of food matrices has been widely investigated (Ju et al., 2019; Ribeiro-Santos, Andrade, Ramos de Melo, & Sanches-Silva, 2017). However, the use of EOs is severely hindered by two main drawbacks. Their high volatility and sensitivity to oxygen and light decrease EOs' stability during processing and storage, eventually impairing their functional and economic efficiency. EO encapsulation is a powerful strategy that overcomes these limitations by controlling the release of the encapsulated agent through the degradation of the embedding material while enhancing the EO's physical stability (Reineccius, 2019; Anal, Shrestha, & Sadiq, 2019). Although surfactants have been used extensively to decrease the interfacial tension in emulsions, new approaches that envision the use of nanoparticles as stabilizers have emerged in recent years (Wu, Luo, & Wang, 2012; Zhang et al., 2012; Jimenez et al., 2014; Campos et al., 2018; Silva et al., 2019). Emulsions stabilized by solid colloidal nanoparticles are referred to as Pickering emulsions. The solid particles are adsorbed onto the oil–water interface, forming long-term steric protection that is mechanically effective against droplet–droplet coalescence (Dickinson, 2019; Hu, Ballinger, Pelton, & Cranston, 2015). Previous studies demonstrated that spherical, rod-like, and plate-like particles can be used to obtain Pickering emulsions. For example, cellulose nanofibrils (Zhang et al., 2020; Li et al., 2019); protein nanoparticles from peanuts (Ning et al., 2020), soy (Ju et al., 2020), gelatin (Ding et al., 2019), ovotransferrin (Wei, Cheng, & Huang, 2019), and hordein (Boostani et al., 2020); dietary fibers (He, Zhang, Li, Li, & Liu, 2020); polysaccharide nanoparticles (Yang, Liu, Li, & Tang, 2019); and polysaccharide/protein complex nanoparticles (Ma, Zou, McClements, & Liu, 2020; Sun, Zhao, Liu, Li, & Li, 2019; Li et al., 2019) have recently been used.

Gelatin has received extensive attention in the food industry as a surfactant due to its high stabilizing activity and good emulsifying properties (Rostami, Yousefi, Khezerlou, Mohammadi, & Jafari, 2019). While gelatin from mammalian sources has been widely used as a food additive, the use of marine gelatin has increased over the years. The reason for this is twofold: first, there is no risk associated with the use of fish gelatin as far as bovine spongiform encephalopathy (BSE) is concerned; second, fish gelatin meets the requirements of Kosher and Halal dietary regulations (Karim & Bhat, 2009).

Cellulose nanofibrils (CNFs) and nanocrystals (CNCs) derived from plants and bacteria have recently emerged as promising nanoparticles due to their outstanding mechanical, thermal, and gas-barrier properties, which can be profitably exploited in various fields, including medical and biomedical devices, purification and cleaning systems (e.g., membranes), displays, green building materials (e.g., insulating panels), and packaging solutions (Rovera et al., 2018). More recently, it has been pointed out that cellulose nanomaterials such as CNFs and CNCs have the potential to develop emulsions because of their excellent mechanical properties, high aspect ratio, and good wet stability (Zhang et al., 2020). Alike other nonspherical nanoparticles, CNCs can be more efficient in stabilizing emulsions than spherical ones for several reasons. For example, the mechanical properties of CNCs monolayers disclosed an exceptionally high surface modulus even at low surface coverage, resulting in in more elastic monolayers compared to aggregate networks of spherical nanoparticles of the same size (Cherhal, Cousin, & Capron, 2015). Anisotropic particles, such as CNCs, allow lowering the percolation threshold, which is of great importance when providing an interface with mechanical rigidity in order to prevent coalescence (Madivala, Vandebril, Fransaer, & Vermant, 2009). In addition, the simultaneous presence of peripheral hydroxyl groups and crystalline domains suggests that CNCs are significantly amphiphilic and can be involved in both polar and hydrophobic interactions

(Dankovich & Gray, 2011; Lindman, Karlstrom, & Stigsson, 2010). For these reasons, cellulose nanoparticles have been advantageously employed as stabilizers in Pickering emulsions. In previous studies, bacterial cellulose nanocrystals (BCNCs), in particular, have been used to emulsify olive oil (Yan et al., 2017), rice bran oil (Angkuratipakorna, Sripraia, Tantrawonga, Chaiyasitb, & Singkhonrata 2017), cinnamaldehyde, eugenol and limonene (Mikulcova, Bordes, & Kasparkova 2016), oregano essential oil (Zhou et al., 2018), peppermint oil (Kasiri & Fathi, 2018), canola oil (Varanasi et al., 2018), palm oil (Wang et al., 2016), and D-limonene (Wen et al., 2011) through stable Pickering emulsions. However, in these studies the final droplet size was in the range of a few microns, that is, the droplet size was much bigger than the size of the cellulose nanocrystals. This is in line with one distinct disadvantage of relying on the Pickering mechanism for the stabilization of emulsions: it normally involves the formation of rather large (micrometer-sized) droplets (Dickinson, 2019).

In this study, we explored the possibility of preparing cinnamon essential oil (CEO) emulsions using BCNCs with and without fish gelatin, with final nanoscale dimension. The goal was to investigate the effect of BCNCs on the CEO nanodroplets, comparing the stabilization mechanism with that of a conventional Pickering emulsion (i.e., solid particles with smaller size than oil droplets). To this end, we used BCNCs obtained from the acid hydrolysis of bacterial cellulose (BC) produced by *Komagataeibacter sucrofermentans*. Fish gelatin was used as a surfactant, and cinnamon bark served as the source of the EO. The effect arising from the addition of fish gelatin on the CEO nanoemulsions was investigated by means of size, morphology, ζ-potential, and encapsulation efficiency analyses as a function of both pH and EO concentration.

1. Material and methods

1.1. Materials

Type A (i.e., extracted by acid pretreatment) fish gelatin (GelA, Kosher and Halal certified) with a gel strength of 200 Bloom was purchased from Weishardt (Graulhet, France). Cinnamon (*Cinnamomum zeylanicum*) bark EO (E-cinnamaldehye: 70.6%; E-cinnamyl acetate: 5.3%; β-caryophyllene: 5.1%; linalool: 4.2%; eugenol: 3.7%; 1,8-cineole + β-phellandrene: 1.2% by GC-MS) was purchased from Plant Therapy Essential Oils Corporate (Twin Falls, USA). BC was produced by static fermentation using *Komagataeibacter sucrofermentans* DSM 15973 (Leibniz Institute DSMZ-German Collection of Microorganisms and Cell Cultures, Braunschweig, Germany) according to the procedure described elsewhere (Rovera et al., 2018). Sulfuric acid (99% v/v), ethanol (96% v/v), and dialysis tubing cellulose membrane (12 kDa, average flat width 43 mm) were purchased from Sigma-Aldrich-Merck (Milano, Italy).

1.2. BCNCs water dispersion preparation

BCNCs were prepared by acid hydrolysis of BC. In brief, 0.914 g of dry BC was added to 6.226 g of distilled water and 100 g of sulfuric acid (50% w/w, in distilled water). The solid particles were evenly dispersed using a DI 25 basic homogenizer with an S25 N – 18 G dispersing tool (Ika-Werke GmbH & Co, Stanfen, Germany) at 9500 rpm for 3 minutes. The hydrolysis reaction was carried out by stirring at 55ºC for 2 hours at 800 rpm. Afterward, the suspension was centrifuged for 50 minutes at 8000 rpm (5260 rcf or g-force) to facilitate the removal of excess sulfuric acid. After centrifugation, the supernatant was replaced with distilled water. After 5 washing cycles, equal aliquots of the suspension were transferred to two dialysis tubes and placed inside a beaker containing distilled water. The water was replaced every 4 hours until the solution's pH reached 3.5 in one dialysis tube and 5 in the

other. These two pH values were selected to assess the pH influence on the properties of the final emulsions. In particular, based on preliminary trials, pH 3.5 was the lowest pH limit to keep the emulsion stable (i.e., with no visible phase separation) over time. The highest value (pH 5) was selected as a reference value (Wang et al., 2016). At this point, the BCNC water dispersions were put in a beaker and ultrasonicated for 5 minutes using a UP200St ultrasonicator (200 W, 26 kHz – Hielscher, Teltow, Germany) mounted with an S26d7D titanium sonotrode (surface area 42 mm^2) at approximately 20 W (pulse: 25%, amplitude 30%) to achieve full nanocrystal dispersion. Final water dispersions (BCNC concentration of 0.4% w/w) were stored at 4°C before further preparation.

1.3. CEO emulsion preparation

To evaluate the influence of CEO concentration and pH on the emulsion's final properties, 2.25 g of BCNC suspension (BCNC concentration 0.4% w/w) at pH 3.5 and 5 (Fig. 1a) was added to various amounts of CEO (4.5, 9, 18, 36, 54, 72 µL). Hence, a series concentration of CEO at 0.2, 0.4, 0.8, 1.57, 2.34 and 3.1% v/w was obtained, then emulsified using the same ultrasonicator as before for 5 minutes at 40 W (pulse: 25%, amplitude 60%) in an ice bath to prevent sample overheating (Fig.1b).

1.4. Addition of fish gelatin to CEO emulsion

A stock solution (10% w/w) of fish gelatin was prepared by adding the gelatin powder to distilled water and heating the mixture to 60ºC under constant stirring (800 rpm) for 2 hours. Then, 8.25 g of distilled water (60°C) was added to six vials, each containing 4.5 g of the stock solution. After decreasing the temperature to 40°C, 2.25 g of each CEO emulsion was added dropwise into the six gelatin solutions at a 0.5 mL/min rate by means of a 10 mL disposable syringe mounted on a syringe pump (mod. NE 1000, New Era Pump Systems Inc.,

USA). The emulsion was then stirred for 15 minutes at 1000 rpm. The final emulsions (15 g) included BCNCs and gelatin at a concentration of 0.06% w/w and 3% w/w, respectively, while the final CEO concentrations were 0.03, 0.06, 0.12, 0.24, 0.36, and 0.48% v/w (Fig. 1c).

1.5. Characterization of BCNCs, CEO/BCNC emulsions, and CEO/BCNC emulsions after the addition of gelatin (CEO-GelA/BCNC).

1.5.1. Particle size, polydispersity index and ζ-potential

The size distribution and polydispersity index (PDI) of BCNCs and droplets in the emulsions were measured using a Nanotrac Flex analyzer based on 180° heterodyne dynamic light scattering (DLS, Microtrac, Montgomeryville, USA). A Litesizer™ 500 (Anton Paar, Rivoli, Italy) was used to measure the ζ-potential of BCNC water dispersions and the emulsions. Before the DLS analysis, a 1/100 (w/w) dilution in phosphate-citrate buffer (0.05 M, pH = 5) was performed for the CEO/BCNC emulsions, and a 1/20 (w/w) dilution in the same buffer was performed for the CEO/BCNC emulsions in the presence of gelatin. A dilution of 1/15 (w/w) with phosphate-citrate buffer (0.05 M, pH = 5) was performed for both emulsions before the ζ-potential measurements. All measurements were conducted in triplicate at 25 ± 0.5°C.

1.5.2. Transmission electron microscopy

Transmission electron microscopy (TEM) was used to observe the morphological features of BCNCs and CEO/BCNC emulsions (e.g., size and droplet coverage) with and without gelatin. A LEO 912 AB energy-filtering transmission electron microscope (Zeiss, Oberkochen, Germany) operating at 80 kV was used to capture the images. Digital images were recorded with a ProScan 1K Slow-Scan CCD camera (ProScan, Scheuring, Germany).

Samples for the TEM analyses were prepared according to the negative staining technique by drop-casting 10 µL of dispersion (1/10 dilution) onto a glow discharged Formvar-coated Cu grid (400-mesh), letting the samples rest for 5 minutes, then blotting the excess of suspension and contrasting with uranyl acetate (2% w/v in water).

1.5.3. Encapsulation efficiency

The encapsulation efficiency (EE) of the CEO/BCNC and CEO-GelA/BCNC emulsions was measured spectrophotometrically using a Lambda 650 UV-visible spectrophotometer (PerkinElmer Inc., Waltham, USA) according to a slightly modified version of the method proposed by Jiulin et al. (2015) and Silva et al. (2018). Emulsions were centrifuged at 12000 rpm (7890 rcf or g-force) for 30 minutes to separate the nanoparticles and the liquid phase. The supernatant was then transferred into Falcon tubes covered with aluminum foil. The absorbance of the supernatant at 287 nm was recorded and inserted into the regression equation of the standard curve, y = 11.258 x (R^2 = 0.9915), which was obtained using a series of known CEO concentrations in the range 5-50 µL/L. The EE was determined using the following equation:

$$\mathrm{EE}(\%) = \left[\frac{W - C \times V}{W}\right] \times 100 \quad (1)$$

where W (g) is the total amount of encapsulated CEO, C (g/mL) is the concentration of CEO in the supernatant, and V (mL) is the total volume of the emulsion.

2. Results and Discussion

2.1. Characterization of BCNCs

Table 1 displays the average size (length, nm), PDI, and ζ-potential (mV) of BCNCs at pH 3.5 and 5. Previous studies on the acid hydrolysis of BC using H_2SO_4 reported an average

length of approximately 855 nm (Kalashnikova, Bizot, Cathala, & Capron, 2011), 290 ± 130 nm (George & Siddaramaiah, 2012), 260 nm (Yan et al., 2017), and from 231 to 296.5 nm (Singhsa, Narain, & Manuspiya 2018). Our results (approximately 320 nm) are in line with the literature, and differences are ascribable to different experimental procedures (e.g., time of hydrolysis and concentration of the acid). Interestingly, there was no statistically significant difference in size between BCNCs stored at pH 3.5 and pH 5, suggesting that the pH values did not change the nanocrystals' state of aggregation.

Concerning the ζ-potential, highly negative values are expected for H_2SO_4-hydrolized BCNCs due to the presence of the sulfate ($-SO_3^-$) groups along the molecular backbone (Lu & Hsieh, 2010). In this study, ζ-potential values of -25.6 ± 0.91 and -27.72 ± 0.16 were obtained for BCNCs stored at pH 3.5 and pH 5, respectively. The more negative ζ-potential values recorded at higher pH values are in line with the decreased concentration of H^+ ions due to an extended dialysis process.

Our values are in line with previous works. Singhsa et al. (2018) reported BCNC ζ-potential values slightly lower than -30 mV, which can be explained by the fact that they continued the dialysis process until neutrality. Yan et al. (2017) reported BCNC emulsion ζ-potential values of about -34.8 mV. This emulsion was derived from carboxyl groups introduced by oxidation on the pyranose ring mediated by hydrogen peroxide. The ζ-potential values obtained in this work are negative enough to generate a sufficient electrostatic repulsion to prevent the aggregation of BCNCs, hence their adequate dispersibility and stability in water.

2.2. Effect of pH and CEO concentration on the size and ζ-potential of emulsions

Various parameters such as oil/water ratio, pH, particle concentration, and solid particles concentration affect the stability of emulsions prepared in the presence of solid nanoparticles

(Leal-Calderon, Thivilliers, & Schmitt, 2007). Oil and solid particle concentrations in particular affect the size of the droplets and their stability to coalescence (Aveyard, Binks, & Clint, 2003). In addition, pH plays an important role in adjusting electrostatic interactions between adjacent nanoparticles at the oil–water interfaces (Zoppe, Venditti, & Rojas, 2012). In this work, the average particle size obtained by DLS increased when the CEO concentration increased for both emulsions (with and without gelatin) (Fig.2a and b). This trend, which is in agreement with the results reported by Cherhal, Cousin, & Capron (2015), Mikulcova et al. (2016.), Yan et al. (2017), and Zhou et al. (2018), can be explained by the increase in the droplets' interfacial area due to the increased CEO concentration. Because the amount of BCNCs was the same for all the formulations, less cellulose is available to stabilize the interfacial area. Hence, an increase in the CEO concentration would lead to a less extensive coverage of the surface of the droplets by the available BCNCs, resulting in an increase of the droplet volume in order to decrease the total interfacial area.

In the case of the emulsions encapsulated in gelatin (Fig. 2b), a marked increase in the droplet size occurred at the lowest pH (3.5). This can be tentatively explained by the isoelectric point (pI) of type A gelatin, which is approximately 8.5 (Duthen et al., 2018; Farris, Cozzolino, Introzzi & Piergiovanni, 2009). At the lowest pH used in this work (3.5), the higher positive charge density on the gelatin backbone is expected promote a more intense unfolding of the protein due to electrostatic repulsion between positively-charged amino groups of lysine (Schrieber & Gareis, 2007). In turn, this would positively affect the coverage of CEO nanoparticles by gelatin, with an ultimate increased size (diameter) of the spherical nanoparticles.

TEM images (Fig. 3) showed that in the absence of gelatin (Figure 3a), some CEO nanodroplets were partially covered by BCNCs via random jammed packing (Kalashnikova, Bizot, Bertonini, Cathala, & Capron, 2013). However, some other particles (especially the

smallest ones) were not adequately surrounded by BCNCs, due to the hindrance caused by the bigger size of the solid particles compared to the CEO nanoparticles. This represents a distinctive difference between the emulsion prepared in this study and a conventional Pickering emulsion. In the presence of fish gelatin (Figure 3b), it was possible to visualize the successful coverage of CEO by gelatin (see the dark shell around the nanodroplets), with BCNCs forming a cage-like structure around the CEO-GelA complex. It can be thus highlighted the amphiphilic behavior of gelatin, which acted as a surfactant by interacting with BCNCs most likely through polar interactions (e.g., electrostatic and dipole-dipole forces) and CEO by weak dispersive forces (e.g., van der Waals interactions). From TEM images, it was also possible to confirm the overall larger size observed for CEO-GelA/BCNC emulsions. Under this scenario, it can be highlighted that BCNCs and gelatin played a different role toward the CEO nanoemulsion. On the one hand, gelatin acted as a true emulsifier, forming a continuous shell around CEO nanoparticles that stabilized the emulsion by both reducing the interfacial tension and acting as a physical barrier to coalescence. At the same time, gelatin layer can be seen as a protective barrier against light and oxygen (Farris, Introzzi & Piergiovanni, 2009), which may represent two main factors of degradation of the essential oil. On the other hand, the outer BCNCs acted more like a scaffold around the CEO-GelA droplets, contributing to the stability of the emulsion by preventing gravitational separation of CEO droplets (i.e., creaming). However, BCNCs did not contribute to protect the CEO nanoemulsion (e.g., against light and oxygen) due to uneven coverage (Figure 3c).

Compared to previous studies, we were able to produce emulsions in the presence of BCNCs with an overall smaller size. Kalashnikova, Bizot, Cathala, & Capron (2011) reported a minimum average diameter of approximately 4 µm; Wen et al. (2011) obtained an average size of 4.2 µm and 6.9 µm; Cherhal et al. (2015) obtained particles of approximately 4 µm, and Wang et al. (2016) reported an average size of approximately 3 µm; Angkuratipakorn et

al. (2017) obtained particles with a minimum diameter of 4.45 µm; Laitinen, Ojala, Sirvio, & Liimatainen, (2017) reported droplet sizes between 7 µm and 10 µm, whereas the size of the particles obtained by Yan et al. (2017) ranged between 5 µm and 15 µm; Varanasi et al. (2018) obtained two groups of particles with sizes of 2.5 µm and 2.7 µm, respectively, whereas Zhou et al. (2018) measured an average droplet diameter of 1.2 µm and 2.9 µm. To explain these values, it must be considered that in all the studies mentioned above, a much higher volume of oil was used to prepare the final Pickering emulsions. In this study, the lower volume of CEO led to nano-sized particles smaller than the BCNCs, differently than what would occur in a typical Pickering emulsion. This is also the reason why the mechanism underlying the stabilization of the CEO emulsion by BCNCs is different from a conventional Pickering emulsion, as described before.

Fig. 4 shows the influence of CEO concentration on the ζ-potential of CEO/BCNC (Fig. 4a) and CEO-GelA/BCNC (Fig. 4b) emulsions at pH values of 3.5 and 5. For both systems (CEO/BCNC and CEO-GelA/BCNC) and for a same pH, an increase in CEO concentration caused no statistically significant change in ζ-potential, which can be ascribed to the nonpolar and uncharged nature of the EO. In addition, for both CEO/BCNC (Fig. 4a) and CEO-GelA/BCNC (Fig. 4b) emulsions it was possible to observe that the ζ-potential evolution at the two different pH values followed the same trend, with the experimental points obtained for the lower pH (3.5) shifted toward more positive values. This reflects the different charge properties of BCNCs prepared at the two different pH values, with more positive ζ-potential values at pH 3.5. (see Table 1). Finally, if we compare the two emulsion types (i.e., with and without fish gelatin), the presence of gelatin in the BCNC emulsion led to a dramatic increase in the ζ-potential to positive values, as can be observed by comparing the plots in Fig. 4a and b. This marked increase can be explained by the extensive positive charge along the gelatin molecules at acidic pH values (a pI value of approximately 8.5 for

type A gelatin), especially at pH 3.5 (hence the higher ζ-potential values at pH 3.5 than at pH 5). However, the positive ζ-potential is much less than 30 mV, which implies a theoretical lower stability for CEO-GelA/BCNC emulsions than CEO/BCNC emulsions. However, both systems (CEO/BCNCs and CEO-GelA/BCNCs) proved stable for 30 days at 42°C, as shown by the digital camera images displayed in Figure S1. It must also be noted that, from a practical point of view, the stability of the CEO-GelA/BCNCs is somehow preserved by the sol-gel transition of the gelatin-based emulsions on cooling (that is, from approximately 40°C to room temperature). During this transition, the gelatin chains partially recover the original triple-helix structure of collagen through a disorder–order rearrangement (Farris, Schaich, Liu, Piergiovanni, & Yam, 2009). This transition takes place within a few hours, during which the emulsions encapsulated with gelatin are stable (no phase separation was visually observed throughout the experiments before solidification). At the same time, this transition is reversible and the original conditions can be restored on melting for temperatures slightly above 40°C.

The effect of CEO concentration and pH on the EE is shown in Fig. 5. For CEO/BCNC and CEO-GelA/BCNC emulsions, an overall EE increase from approximately 30-40% up to 80% was observed as a function of CEO concentration. In particular, for both emulsion systems (i.e., CEO/BCNCs and CEO-GelA/BCNCs) the EE increased steeply in correspondence of the two lowest CEO concentrations, and eventually reached a linear trend at the highest CEO concentration. This seems in contrast to previous works in which gelatin was used to encapsulate essential oils (Jiulin et al., 2015; Silva et al., 2018). We are prone to consider this deviation from the non-linearity as a consequence of the centrifugation step, which plausibly was not able to separate adequately the finest (smallest) emulsion droplets that remained in the main continuous phase. In practice, this would lead to an

underestimation of the EE for the lowest CEO concentrations (0.2 and 0.4% v/w for the CEO/BCNC emulsions and 0.03 and 0.06% v/w for the CEO-GelA/BCNCs emulsions).

The effect of pH on EE was not statistically significant for the CEO/BCNC emulsions. This suggests that BCNCs' ability to entrap the oil droplets was not affected by pH, probably because this change did not significantly affect the system's overall stability (see the ζ-potential values in Fig. 4). On the contrary, a significant effect of pH on EE was observed for the emulsions stabilized with gelatin up to a CEO concentration of 0.24% v/w, with the highest EE values determined at the highest pH. In line with our previous discussion, the fact that this significant difference concerned the non-linear part of the EE evolution suggests that the recovery of CEO by centrifugation was probably more effective at pH 5, i.e., for the highest negative charge density on the BCNCs and the lowest positive charge density of gelatin. This seems to be corroborated by the fact that: i) as discussed before, coverage of CEO droplets by gelatin is less effective at pH 5; ii) CNCs with higher surface charge density form less stable emulsions (Kalashnikova, Bizot, Cathala, & Capron, 2012).

3. Conclusions

In this study, oil-in-water emulsions were prepared using CEO and BCNCs. The stability of the CEO/BCNC emulsions was successfully achieved through both electrostatic repulsion (ζ-potential values of approximately -25 mV) and the entrapment of the oil droplets in BCNCs scaffolds that primarily prevented creaming. The addition of gelatin led to a different scenario, with the protein acting as a surfactant that adsorbed onto the oil surface fully covering the CEO nanodroplets and offered steric protection against oil droplet coalescence even after 30 days. This study's findings can be used profitably in the food industry to design new systems that can benefit from the effect arising from a conventional surfactant and solid nanoparticles of biological origin. This type of systems might function as carriers of

encapsulated bioactive compounds mixed directly into the food matrix or as films and coatings.

Declaration of competing interest

All authors have no competing interest to declare.

Acknowledgments

Mahsa Razavi is grateful to the Ministry of Science, Research and Technology of Iran for financial support during her stay at the University of Milan.

References

Anal, A. K., Shrestha, S., & Sadiq, M. B. (2019). Biopolymeric-based emulsions and their effects during processing, digestibility and bioaccessibility of bioactive compounds in food systems. *Food Hydrocolloids*, *87*, 691–702. https://doi.org/10.1016/j.foodhyd.2018.09.008

Angkuratipakorna, T., Sripraia, A., Tantrawonga, S., Chaiyasitb, W., & Singkhonrata, J., (2017). Fabrication and characterization of rice bran oil-in-water Pickering emulsion stabilized by cellulose nanocrystals. *Colloids and Surfaces A: Physicochemical and Engineering Aspects*, *522*, 310–319. http://dx.doi.org/10.1016/j.colsurfa.2017.03.014

Aveyard, R., Binks, B. P., & Clint, J. H. (2003). Emulsions stabilised solely by colloidal particles. *Advances in Colloid and Interface Science*, *100–102*, 503–546. http://dx.doi.org/10.1016/S0001-8686(02)00069-6

Boostani, S., Hosseini, S. M. H., Golmakani, M. T., Marefati, A., Hadi, N. B. A., & Rayner, M. (2020). The influence of emulsion parameters on physical stability and rheological properties of Pickering emulsions stabilized by hordein nanoparticles. *Food Hydrocolloids*, *101*, 105520. https://doi.org/10.1016/j.foodhyd.2019.105520

Cherhal, F., Cousin, F., & Capron, I. (2015). Structural description of the interface of Pickering emulsions stabilized by cellulose nanocrystals. *Biomacromolecules*, *17*, 496–502. https://doi.org/10.1021/acs.biomac.5b01413

Campos, E. V. R., Proença, P. L. F., Oliveira, J. L., Pereira, A. E. S., de Morais Ribeiro, L. N., Fernandes, F. O., Gonçalves, K. C., Polanczyk, R. A., Pasquoto-Stigliani, T., Lima, R., Melville, C. C., Della Vechia, J. F., Andrade, D. J., & Fraceto, L. F. (2018). Carvacrol and linalool co-loaded in β-cyclodextrin-grafted chitosan nanoparticles as sustainable biopesticide aiming pest control. *Scientific Reports*, *8*, 7623. https://doi.org/10.1038/s41598-018-26043-x

Dankovich, T. A., & Gray, D. G. (2011). Contact angle measurements on smooth nanocrystalline cellulose (I) thin films. *Journal of Adhesion Science and Technology, 25*, 699–708. https://doi.org/10.1163/016942410X525885

Dickinson, E. (2019). Strategies to control and inhibit the flocculation of protein-stabilized oil-in-water emulsions. *Food Hydrocolloids*, *96*, 209–223. https://doi.org/10.1016/j.foodhyd.2019.05.021

Duthen, S., Rochat, C., Kleiber, D., Violleau, F., Daydé, J., Raynaud, C., & Levasseur-Garcia, C. (2018). Physicochemical characterization and study of molar mass of industrial gelatins by AsFlFFF-UV/MALS and chemometric approach. *PLoS ONE*, *13*, e0203595. https://doi.org/10.1371/journal.pone.0203595

Ding, M., Zhang, T., Zhang, H., Tao, N., Wang, X., & Zhong, J. (2019). Effect of preparation factors and storage temperature on fish oil-loaded crosslinked gelatin nanoparticle Pickering emulsions in liquid forms. *Food Hydrocolloids*, *95*, 326–335. https://doi.org/10.1016/j.foodhyd.2019.04.052

Farris, S., Introzzi, L., & Piergiovanni L. (2009) Evaluation of a bio-coating as a solution to improve barrier, friction and optical properties of plastic films. *Packaging Technology and Science, 22*, 69-83. https://doi.org/10.1002/pts.826

Farris, S., Cozzolino, C. A., Introzzi, L., & Piergiovanni, L. (2009). Effects of different sealing conditions on the seal strength of polypropylene films coated with a bio-based thin layer. *Packaging Technology & Science*, *22*, 359–369. https://doi.org/10.1002/pts.861

Farris, S., Schaich, K. M., Shu, L., Piergiovanni, L., & Yam, K. L. (2009). Development of polyion-complex hydrogels as an alternative approach for the production of bio-based

polymers for food packaging applications: a review. *Trends in Food Science & Technology*, *20*, 316–332. https://doi.org/10.1016/j.tifs.2009.04.003

George, J., & Siddaramaiah, (2012). High performance edible nanocomposite films containing bacterial cellulose nanocrystals. *Carbohydrate Polymers*, *87*, 2031–2037. https://doi.org/10.1016/j.carbpol.2011.10.019

He, K., Zhang, X., Li, Y., Li, B., & Liu, S. (2020). Water-insoluble dietary-fibers from *Flammulina velutiper* used as edible stabilizers for oil-in-water Pickering emulsions. *Food Hydrocolloids*, *101*, 105519. https://doi.org/10.1016/j.foodhyd.2019.105519

Hu, Z., Ballinger, S., Pelton, R., & Cranston, E. D. (2015). Surfactant-enhanced cellulose nanocrystal Pickering emulsions. *Journal of Colloid and Interface Science*, *439*, 139–148. https://doi.org/10.1016/j.jcis.2014.10.034

Jiang, C., Shi, J., Liu, Y., & Zhu, C., (2014). Inhibition of *Aspergillus carbonarius* and fungal contamination in table grapes using *Bacillus subtilis*. *Food Control*, *35*, 41–48. https://doi.org/10.1016/j.foodcont.2013.06.054

Jimenez, A., Sanchez-Gonzalez, L., Desobry, S., Chiralt, A., & Arab Tehrany, E. (2014). Influence of nanoliposomes incorporation on properties of film forming dis- persions and films based on corn starch and sodium caseinate. *Food Hydrocolloids*, *35*, 159–169. https://doi.org/10.1016/j.foodhyd.2013.05.006

Jiulin, W., Liu, H., Ge, S., Wang, S., Qin, Z., Chen, L., Zheng, Q., Liu, Q., & Zhang, Q. (2015). The preparation, characterization, antimicrobial stability and in vitro release evaluation of fish gelatin films incorporated with cinnamon essential oil nanoliposomes. *Food Hydrocolloids*, *43*, 427–435. http://dx.doi.org/10.1016/j.foodhyd.2014.06.017

Ju, J., Chen, X., Xie, Y., Yu, H., Guo, Y., Cheng., Y., Qian, H., & Yao, W. (2019). Application of essential oil as a sustained release preparation in food packaging. *Trends in Food Science & Technology, 92*, 22–32. https://doi.org/10.1016/j.tifs.2019.08.005

Ju, M., Zhu, G., Huang, G., Shen, X., Zhang, Y., Jiang, L., & Sui, X. (2020). A novel Pickering emulsion produced using soy protein-anthocyanin complex nanoparticles. *Food Hydrocolloids*, *99*, 105329. https://doi.org/10.1016/j.foodhyd.2019.105329

Karim, A. A. & Bhat, R. (2009). Fish gelatin: properties, challenges, and prospects as an alternative to mammalian gelatins. *Food Hydrocolloids, 23*, 563–576. https://doi.org/10.1016/j.foodhyd.2008.07.002

Kalashnikova, I., Bizot, H., Cathala, B., & Capron, I. (2011). New Pickering emulsions stabilized by bacterial cellulose nanocrystals. *Langmuir*, *27*, 7471−7479. https://doi.org/10.1021/la200971f

Kalashnikova, I., Bizot, H., Cathala, B., & Capron, I. (2012). Modulation of cellulose nanocrystals amphiphilic properties to stabilize oil/water interface. *Biomacromolecules, 13*, 267−275. https://doi.org/10.1021/bm201599j

Kalashnikova, I., Bizot, H., Bertonini, P., Cathala, B., & Capron, I. (2013). Cellulosic nanorods of various aspect ratios for oil in water Pickering emulsions. *Soft Matter, 9*, 952−959. https://doi.org/10.1039/c2sm26472b

Kasiri, N., & Fathi, M. (2018). Entrapment of peppermint oil using cellulose nanocrystals. *Cellulose*, *25*, 319–329. https://doi.org/10.1007/s10570-017-1574-5

Laitinen, O., Ojala, J., Sirvio, J. A., & Liimatainen, H. (2017). Sustainable stabilization of oil in water emulsions by cellulose nanocrystals synthesized from deep eutectic solvents. *Cellulose*, *24*, 1679–1689. https://doi.org/10.1007/s10570-017-1226-9

Leal-Calderon, F., Thivilliers, F., & Schmitt, V. (2007). Structured emulsions. *Current Opinion in Colloid & Interface Science*, *12*, 206–212. https://doi.org/10.1016/j.cocis.2007.07.003

Li, Q., Xie, B., Wang, Y., Wang, Y., Peng, L., Li, Y., Li, B., & Liu, S. (2019). Cellulose nanofibrils from *Miscanthus floridulus* straw as green particle emulsifier for O/W Pickering emulsion. *Food Hydrocolloids*, *97*, 105214. https://doi.org/10.1016/j.foodhyd.2019.105214

Li, M.-F., He, Z.-Y., Li, G.-Y., Zeng, Q.-Z., Su, D.-X., Zhang, J.-L., Wang, Q., Yuan, Y., & He, S. (2019). The formation and characterization of antioxidant Pickering emulsions: Effect of the interactions between gliadin and chitosan. *Food Hydrocolloids*, *90*, 482–489. https://doi.org/10.1016/j.foodhyd.2018.12.052

Lindman, B., Karlstrom, G., & Stigsson, L. (2010). On the mechanism of dissolution of cellulose. *Journal of Molecular Liquids*, *156*, 76–81. https://doi.org/10.1016/j.molliq.2010.04.016

Lu, P., & Hsieh, Y. L. (2010). Preparation and properties of cellulose nanocrystals: Rods, spheres, and network. *Carbohydrate Polymers*, *82*, 329−336. https://doi.org/10.1016/j.carbpol.2010.04.073

Ma, L, Zou, L., McClements, D. J., & Liu, W. (2020). One-step preparation of high internal phase emulsions using natural edible Pickering stabilizers: Gliadin nanoparticles/gum arabic. *Food Hydrocolloids*, *100*, 105381. https://doi.org/10.1016/j.foodhyd.2019.105381

Madivala,B., Vandebril, S., Fransaer, J., & Vermant, J. (2009). Exploiting particle shape in solid stabilized emulsions. *Soft Matter*, *5*, 1717–1727. https://doi.org/10.1039/b816680c

Mikulcova, M., Bordes, R., & Kasparkova, V. (2016). On the preparation and antibacterial activity of emulsions stabilized with nanocellulose particles. *Food Hydrocolloids*, *61*, 780–792. http://dx.doi.org/10.1016/j.foodhyd.2016.06.031

Ning, F., Ge, Z., Qiu, L. Wang, X., Luo, L., Xiong, H., & Huang, Q. (2020). Double-induced se-enriched peanut protein nanoparticles preparation, characterization and stabilized food-grade Pickering emulsions. *Food Hydrocolloids*, *99*, 105308. https://doi.org/10.1016/j.foodhyd.2019.105308

Reineccius, G. (2019). Use of proteins for the delivery of flavours and other bioactive compounds. *Food Hydrocolloids*, *86*, 62–69. https://doi.org/10.1016/j.foodhyd.2018.01.039

Ribeiro-Santos, R., Andrade, M., Ramos de Melo, N., & Sanches-Silva, A. (2017). Use of essential oils in active food packaging: Recent advances and future trends. *Trends in Food Science & Technology*, *61*, 132–140. https://doi.org/10.1016/j.tifs.2016.11.021

Rostami, M. R., Yousefi, M., Khezerlou, A., Mohammadi, M. A., & Jafari, S. M. (2019). Application of different biopolymers for nanoencapsulation of antioxidants via electrohydrodynamic processes. *Food Hydrocolloids*, *97*, 105170. https://doi.org/10.1016/j.foodhyd.2019.06.015

Rovera, C., Ghaani, M., Santo, N., Trabattoni, S., Olsson, R. T., Romano, D., & Farris S. (2018). Enzymatic hydrolysis in the green production of bacterial cellulose nanocrystals. *ACS Sustainable Chemistry & Engineering*, *6*, 7725–7734. https://doi.org/10.1021/acssuschemeng.8b00600

Schrieber, R., & Gareis, H. (2007). *Gelatine Handbook: Theory and Industrial Practice*. Weinheim, Germany: Wiley-VCH (p. 61).

Silva, L. S., Mar, J. M., Azevedo, S. G., Rabelo, M. S., Bezerra, J. A., Campelo, P. H., Machado, M. B., Trovati, G., dos Santos, A. L., da Fonseca Filho, H. D., de Souza, D. P., & Sanches, E. A. (2018). Encapsulation of *Piper aduncum* and *Piper hispidinervum* essential oils in gelatin nanoparticles: a possible sustainable control tool of *Aedes aegypti*, *Tetranychus urticae* and *Cerataphis lataniae*. *Journal of the Science of Food and Agriculture*, *99*, 685–695. https://doi.org/10.1002/jsfa.9233

Singhsa, P., Narain, R., & Manuspiya, H., (2018). Bacterial cellulose nanocrystals (BCNC) preparation and characterization from three bacterial cellulose sources and development of functionalized BCNCs as nucleic acid delivery systems. *ACS Applied Nano Materials*, *1*, 209–221. https://doi.org/10.1021/acsanm.7b00105

Sun, G., Zhao, Q., Liu, S., Li, B., & Li, Y. (2019). Complex of raw chitin nanofibers and zein colloid particles as stabilizer for producing stable Pickering emulsions. *Food Hydrocolloids*, *97*, 105178. https://doi.org/10.1016/j.foodhyd.2019.105178

Varanasi, S., Henzel, L., Mendoza, L., Prathapan, R., Batchelor, W., Tabor, R., & Garnier, G., (2018). Pickering emulsions electrostatically stabilized by cellulose nanocrystals. *Frontiers in Chemistry*, *6*, 409. https://doi.org/10.3389/fchem.2018.00409

Wang, W., Du, G., Li, C., Zhang, H., Long, Y., & Ni, Y. (2016). Preparation of cellulose nanocrystals from asparagus (*Asparagus officinalis L.*) and their applications to palm oil/water Pickering emulsion. *Carbohydrate Polymers*, *151*, 1–8. http://dx.doi.org/10.1016/j.carbpol.2016.05.052

Wei, Z., Cheng, J., & Huang, Q. (2019). Food-grade Pickering emulsions stabilized by ovotransferrin fibrils. *Food Hydrocolloids*, *94*, 592–602. https://doi.org/10.1016/j.foodhyd.2019.04.005

Wen, C., Yuana, Q., Lianga, H., & Vriesekoop, F. (2011). Preparation and stabilization of d-limonene Pickering emulsions by cellulose nanocrystals. *Carbohydrate Polymers*, *112*, 695–700. http://dx.doi.org/10.1016/j.carbpol.2014.06.051

Wu, Y., Luo, Y., Wang, Q. 2012. Antioxidant and antimicrobial properties of essential oils encapsulated in zein nanoparticles prepared by liquid-liquid dispersion method. *LWT - Food Science and Technology*, *48*, 283–290. https://doi.org/10.1016/j.lwt.2012.03.027

Yan, H., Chen, X., Song, H., Li, J., Feng, Y., Shi, Z., Wang, X., & Lin, Q. (2017). Synthesis of bacterial cellulose and bacterial cellulose nanocrystals for their applications in the stabilization of olive oil pickering emulsion. *Food Hydrocolloids*, *72*, 127–135. http://dx.doi.org/10.1016/j.foodhyd.2017.05.044

Yang, T., Liu, T.-X., Li, X.-T., & Tang, C.-H. (2019). Novel nanoparticles from insoluble soybean polysaccharides of Okara as unique Pickering stabilizers for oil-in-water emulsions. *Food Hydrocolloids*, *94*, 255–267. https://doi.org/10.1016/j.foodhyd.2019.105574

Zhang, H. Y., Arab Tehrany, E., Kahn, C. J. F., Ponçot, M., Linder, M., & Cleymand, F. (2012). Effects of nanoliposomes based on soya, rapeseed and fish lecithins on chitosan thin films designed for tissue engineering. *Carbohydrate Polymers*, *88*, 618–627. https://doi.org/10.1016/j.carbpol.2012.01.007

Zhang, X., Zhou, J., Chen, J., Li, B., Li, Y., & Liu, S. (2020). Edible foam based on pickering effect of bacterial cellulose nanofibrils and soy protein isolates featuring interfacial network

stabilization. *Food Hydrocolloids, 100,* 105440. https://doi.org/10.1016/j.foodhyd.2019.105440

Zhou, Y., Sun, S., Bei, W., Zahi, M. R., Yuan, Q., & Liang, H. (2018). Preparation and antimicrobial activity of oregano essential oil Pickering emulsion stabilized by cellulose nanocrystals. *International Journal of Biological Macromolecules, 112,* 7–13. https://doi.org/10.1016/j.ijbiomac.2018.01.102

Zoppe, J. O., Venditti, R. A., & Rojas, O. J. (2012). Pickering emulsions stabilized by cellulose nanocrystals grafted with thermo-responsive polymer brushes. *Journal of Colloid and Interface Science, 369,* 202–209. https://doi.org/10.1016/j.jcis.2011.12.011

535 **Figure captions**

536 **Fig. 1.** Addition of CEO in the 6 series concentration BCNCs water dispersions (a),
537 CEO/BCNC emulsions after ultrasonication (b), and CEO/BCNCs emulsions encapsulated in
538 fish gelatin (c). Both emulsions were prepared at pH 3.5. A zoomed image is provided at the
539 left of each panel.

540

541 **Fig. 2.** Evolution of the particle size of CEO/BCNC (a) and CEO-GelA/BCNC (b) emulsions
542 as a function of CEO concentration and at two different pH values.

543

544 **Fig. 3.** (a) Transmission electron microscopy images of CEO/BCNC and (b) CEO-
545 GelA/BCNC emulsions at the highest CEO concentration (3.1 and 0.48% v/w, respectively).
546 Schematic representation of CEO/BCNC emulsion with and without gelatin (c).

547

548 **Fig. 4.** Variation of the ζ-potential of CEO/BCNC (a) and CEO-GelA/BCNC (b) emulsions
549 as a function of CEO concentration and at two different pH values.

550

551 **Fig. 5.** Variation of the encapsulation efficiency (EE) of CEO/BCNC (a) and CEO-
552 GelA/BCNC (b) emulsions as a function of CEO concentration and at two different pH
553 values.

554

555

556

557

Tables

Table 1 Size, polydispersity index and ζ-potential of BCNCs at two different pHs.

pH	Length (nm)	PDI	ζ-potential (mV)
3.5	319.64 ± 16.22^{a}	0.527 ± 0.047^{b}	-25.60 ± 0.91^{c}
5	322.08 ± 30.02^{a}	0.340 ± 0.117^{b}	-27.72 ± 0.16^{d}

Values are reported as average ± standard deviation. The superscripts refer to statistically significant differences within the same group (i.e., within the same parameter) ($p < 0.05$).

Table 1 Size, polydispersity index and ζ-potential of BCNCs at two different pHs.

pH	Length (nm)	PDI	ζ-potential (mV)
3.5	319.64 ± 16.22^{a}	0.527 ± 0.047^{b}	-25.60 ± 0.91^{c}
5	322.08 ± 30.02^{a}	0.340 ± 0.117^{b}	-27.72 ± 0.16^{d}

Values are reported as average ± standard deviation. The superscripts refer to statistically significant differences within the same group (i.e., within the same parameter) ($p < 0.05$).

Figure 1

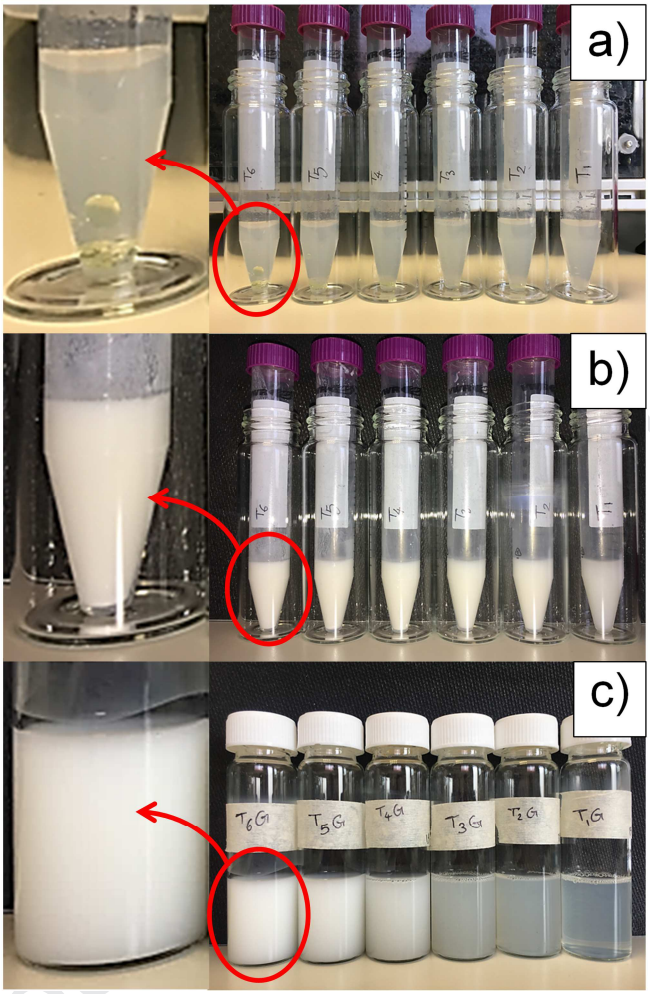

Figure 2

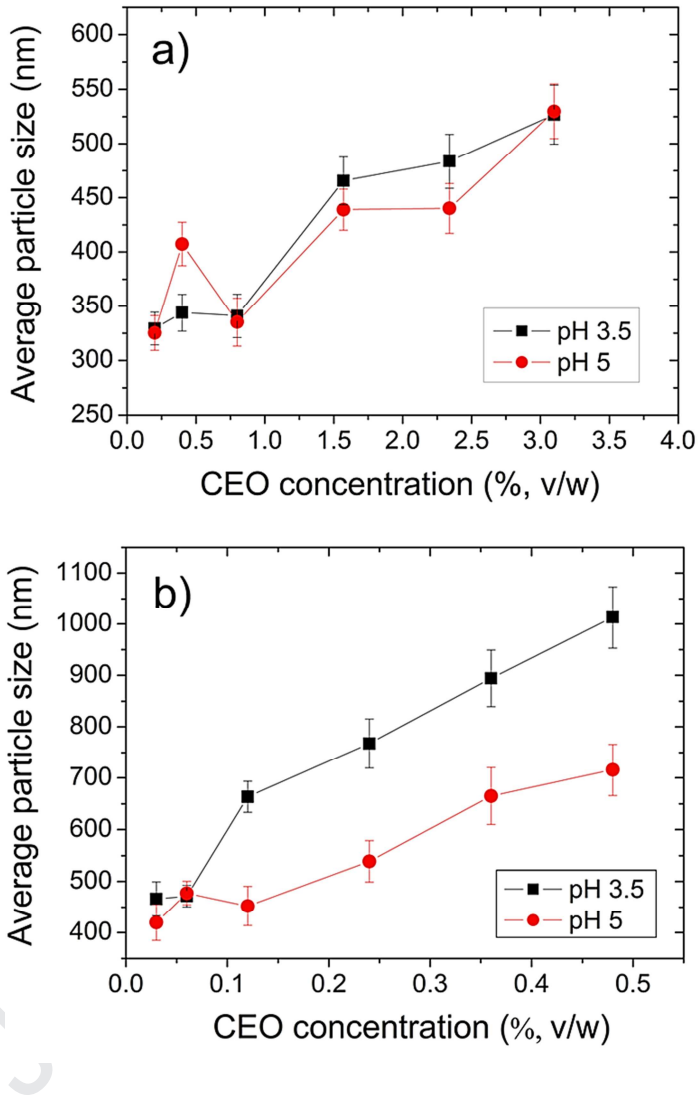
a)
Average particle size (nm)
600
550
500
450
400
350
300
250
0.0
0.5
1.0
1.5
2.0
2.5
3.0
3.5
4.0
CEO concentration (%, v/w)
pH 3.5
pH 5
b)
Average particle size (nm)
1100
1000
900
800
700
600
500
400
0.0
0.1
0.2
0.3
0.4
0.5
CEO concentration (%, v/w)
pH 3.5
pH 5

Figure 3

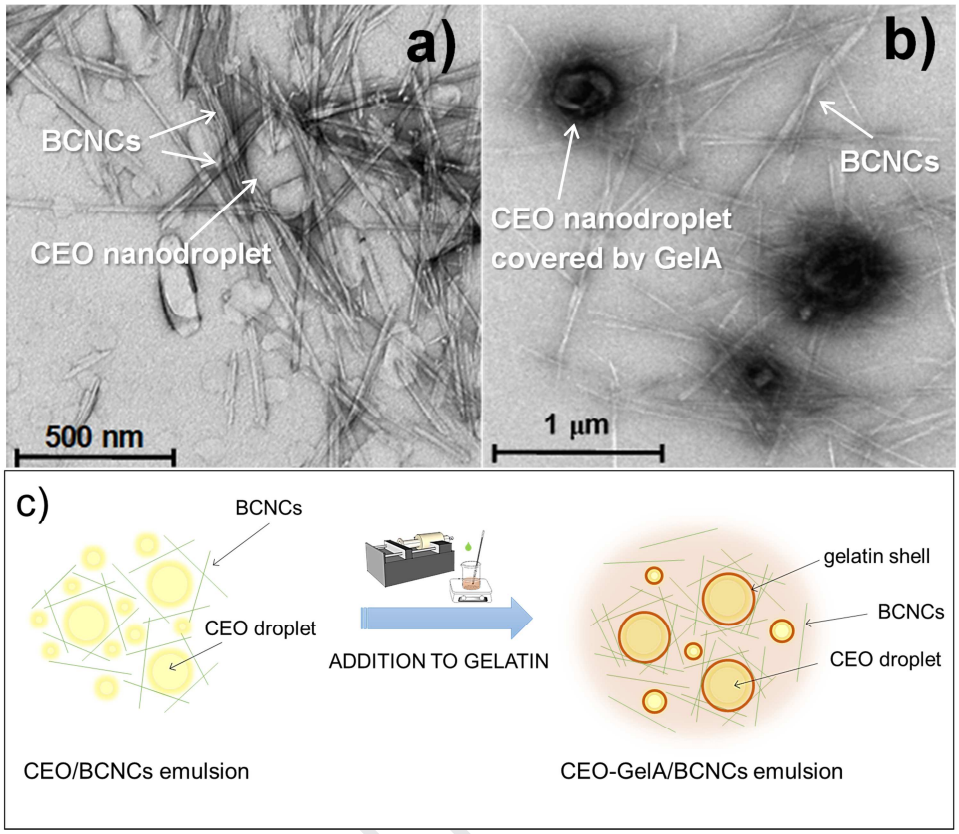

Figure 4

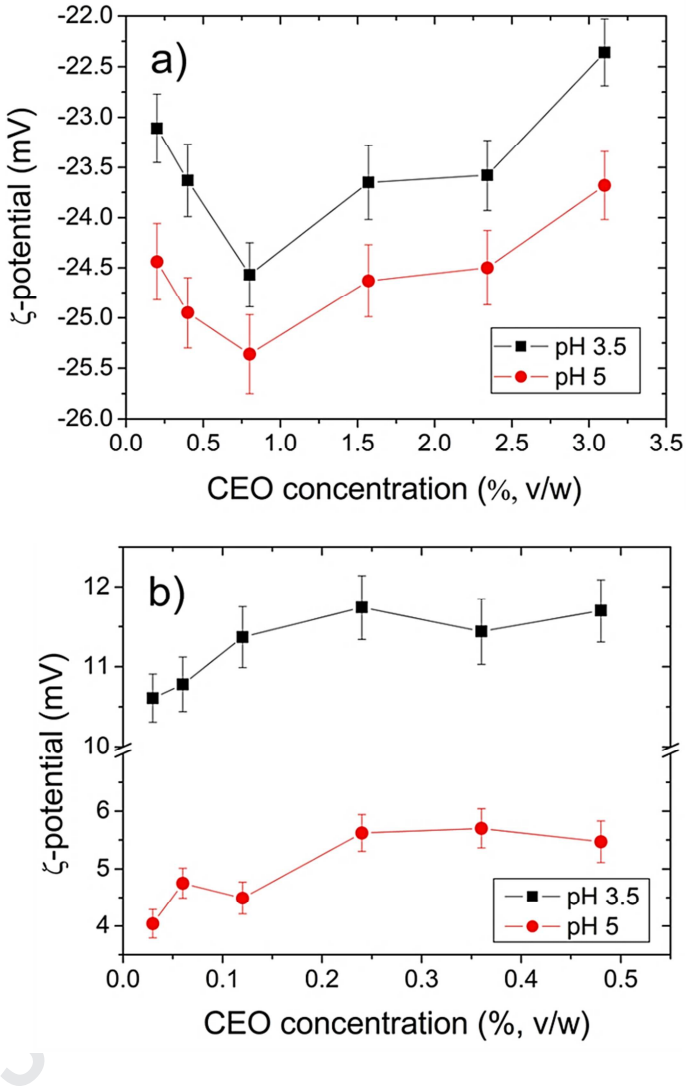
a)
ζ-potential (mV)
-22.0
-22.5
-23.0
-23.5
-24.0
-24.5
-25.0
-25.5
-26.0
0.0
0.5
1.0
1.5
2.0
2.5
3.0
3.5
CEO concentration (%, v/w)
pH 3.5
pH 5
b)
ζ-potential (mV)
12
11
10
6
5
4
0.0
0.1
0.2
0.3
0.4
0.5
CEO concentration (%, v/w)
pH 3.5
pH 5

Figure 5

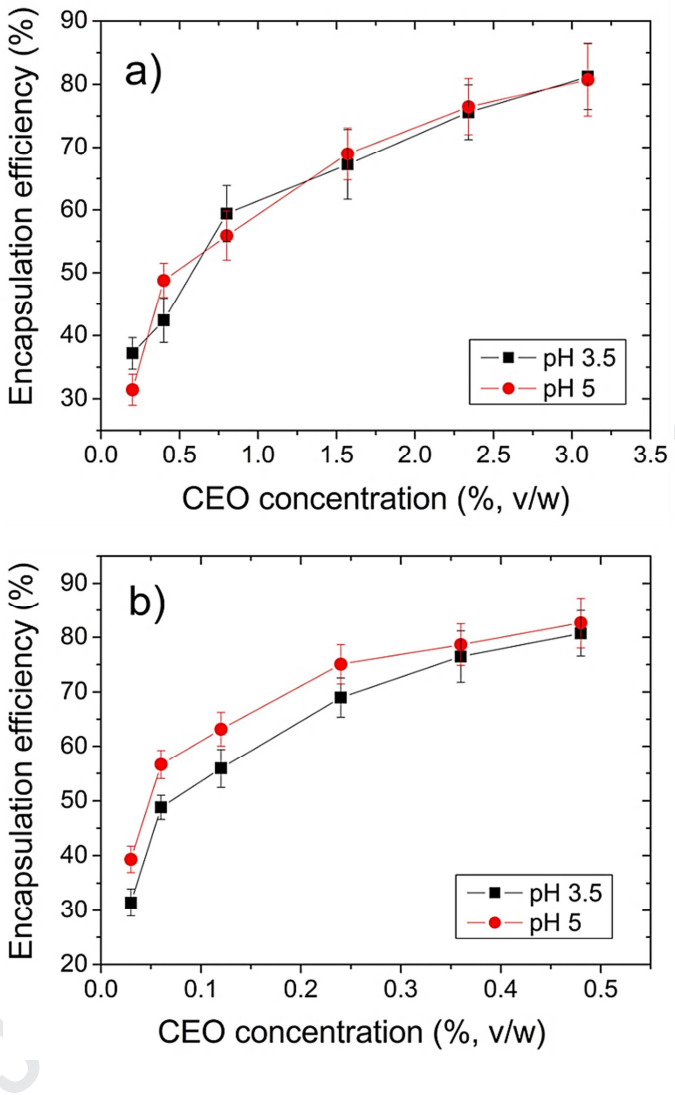
a)
Encapsulation efficiency (%)
CEO concentration (%, v/w)
pH 3.5
pH 5
b)
Encapsulation efficiency (%)
CEO concentration (%, v/w)
pH 3.5
pH 5

Highlights

- An oil-in-water emulsion was obtained using cinnamon essential oil
- Bacterial cellulose nanocrystals (BCNCs) were used as solid nanoparticles
- Emulsions with and without fish gelatin were also prepared
- Oil concentration and pH affected several physical properties of the emulsions
- Nanoemulsions stabilized by gelatin and BCNCs were obtained

Conflict of interest

Declarations of interest: none.

Author statement

Conceptualization: M.R. and S.F.; methodology, M.R. and S.F.; formal analysis, M.F., C.R. and F.F.; investigation, M.F., C.R. and F.F.; writing—original draft preparation, M.R., C.R.; writing—review and editing, A.G., A.N. and S.F.; visualization, S.F.; supervision, S.F. All authors have read and agreed to the published version of the manuscript.